COLLÈGE DE FRANCE
1530

Chaire de Physique de la Matière Condensée

Cuprates supraconducteurs : où en est-on ?

Antoine Georges

Cycle 2010-2011
Cours 5 – 30/11/2010

Cours 5 - 30/11/2010

Cours: Phénoménologie de la phase supraconductrice des cuprates

- 15h30: Alain Sacuto, Université Denis Diderot
  Température critique et appariement dans les oxydes de cuivre supraconducteurs
- 16h45: Jérôme Lesueur, ESPCI
  Une mesure directe des fluctuations supraconductrices dans la phase sous dopée des cuprates.

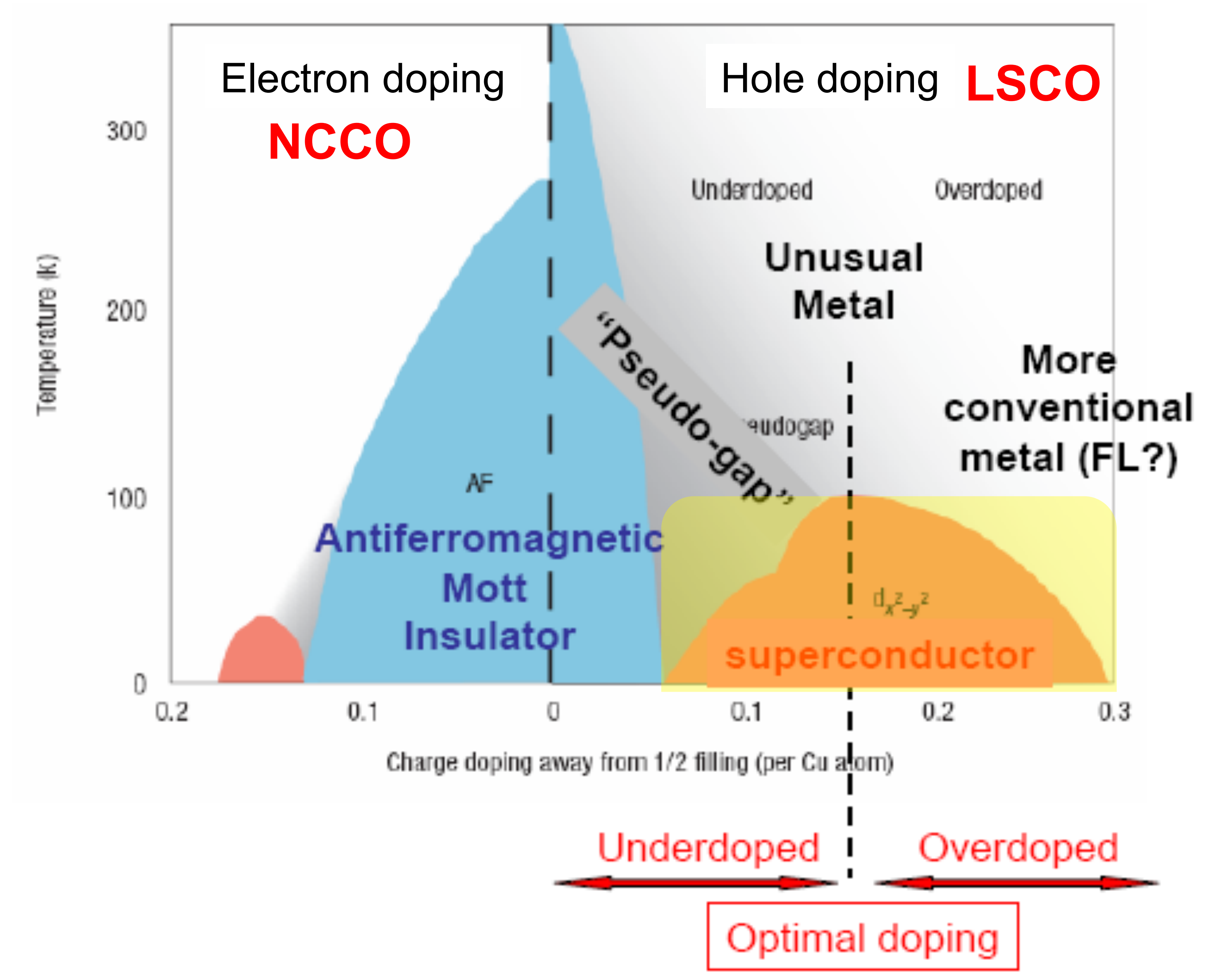

Cuprates: "Generic" phase diagram

From underdoped to overdoped

- Some key properties of the SC phase are generic for all doping regimes
- However, some important differences also stand out between the underdoped and overdoped side
- → *The unusual aspects of the underdoped normal state are not entirely wiped out by SC order (~ contrary to earlier belief)*

1. d-wave symmetry of the SC order parameter

- Singlet-pairing: suppression of Knight-shift below T_c
- Existence of pairs of charge 2e: Early flux quantization experiments $\Phi_0 = hc/2e$
- On-site (local) s-wave pairing is expected to be suppressed by strong Coulomb repulsion
- Indeed, the on-site U will contribute a Hartree/BCS like term to the energy: $\frac{NU}{4}\left\{n^2+\left|\frac{1}{N}\sum_k \frac{\Delta_0(k)}{E_k}\right|^2\right\}$ $E_k = \left[\xi_k^2 + \Delta_k^2\right]^{1/2}$
- → Need to make this term vanish for SC to be favorable
- $\Delta(k)$ must change sign in the BZ

`Extended' s-wave or d-wave ?

$$\Delta_k^{s,A_{1g}} = \Delta_0^s + \Delta_1^s(\cos k_x + \cos k_y) + \text{higher harmonics}$$

has symmetry C_4 of the square lattice (tetragonal symmetry assumed here)

$$\Delta_k^d = \Delta_{B_{1g}}(\cos k_x - \cos k_y) + \quad \leftarrow \text{``}x^2\text{-}y^2\text{'' gap}$$

$$+\Delta_{B_{2g}} \sin k_x \sin k_y + \quad \leftarrow \text{``}xy\text{'' gap}$$

$$+\text{higher harmonics}$$

breaks symmetry of the square lattice

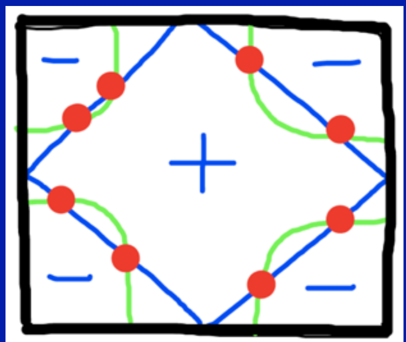

A_{1g} for Δ_0=0

B_{1g}

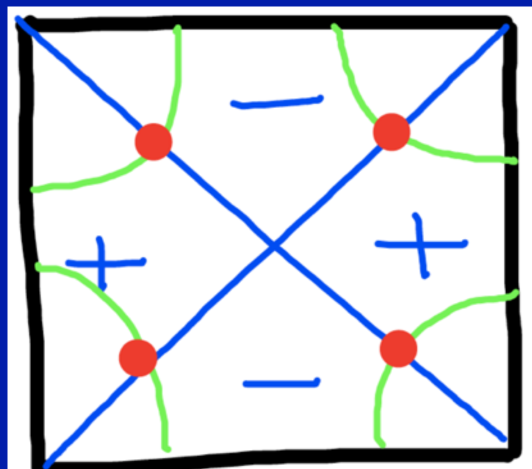

B_{2g}

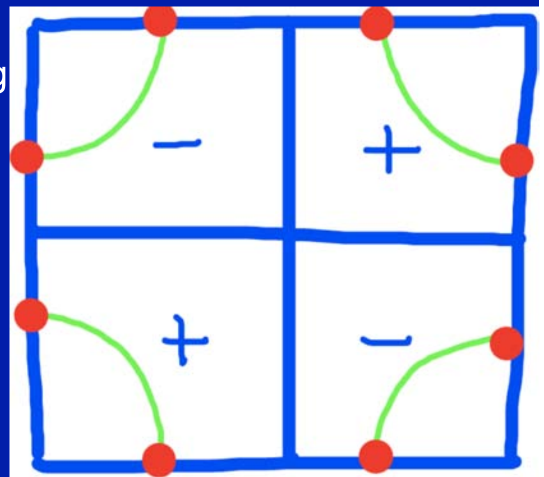

TABLE I. Spin-singlet even-parity pair states in a tetragonal crystal with point group D_{4h}.

Wave-function name	Group-theoretic notation, T_j	Residual symmetry	Basis function	Nodes
s wave	A_{1g}	$D_{4h}\times \mathrm{T}$	$1,(x^2+y^2),z^2$	none
g	A_{2g}	$D_4[C_4]\times C_i\times \mathrm{T}$	$xy(x^2-y^2)$	line
$d_{x^2-y^2}$	B_{1g}	$D_4[D_2]\times C_i\times \mathrm{T}$	x^2-y^2	line
d_{xy}	B_{2g}	$D_4[D_2']\times C_i\times \mathrm{T}$	xy	line
$e_{(1,0)}$	$E_g(1,0)$	$D_4[C_2']\times C_i\times \mathrm{T}$	xz	line
$e_{(1,1)}$	$E_g(1,1)$	$D_2[C_2'']\times C_i\times \mathrm{T}$	$(x+y)z$	line
$e_{(1,i)}$	$E_g(1,i)$	$D_4[E]\times C_i$	$(x+iy)z$	line

From: Tsuei and Kirtley, Rev Mod Phys 72, 969 (2000)

d-wave implies lines of zero-gap and gapless quasiparticle excitations at ``nodal'' k-points
- see below -

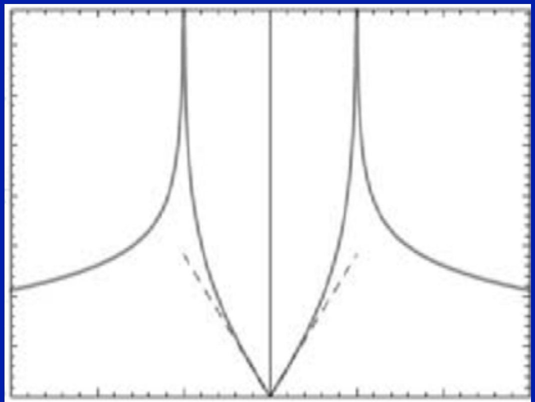

$$E_k = \sqrt{(\varepsilon_k - \mu)^2 + \Delta_k^2}$$

→ $$\xi_k^{QP} \simeq \sqrt{v_F^2\, \delta k_{||}^2 + v_\Delta^2\, \delta k_\perp^2}$$ Dirac cone

$$\boxed{N_{QP}(\varepsilon) = \int \frac{d^2k}{(2\pi)^2}\, \delta(\varepsilon - \xi_k^{QP}) = \frac{1}{2\pi v_F v_\Delta} |\varepsilon|}$$

Linear density of states for nodal QP excitations

→ Response functions/ thermodynamic measurements
Display power-law behavior, which is however characteristic of nodal points on the FS, NOT of precise symmetry of the gap

Example : NMR $1/T_1$

(cf. H.Alloul's seminar)

$1/T_1 \sim T^3$

$$G(\tau) \sim \frac{1}{\tau^2}$$

$$\Rightarrow \chi''(\omega) \sim \omega^3$$

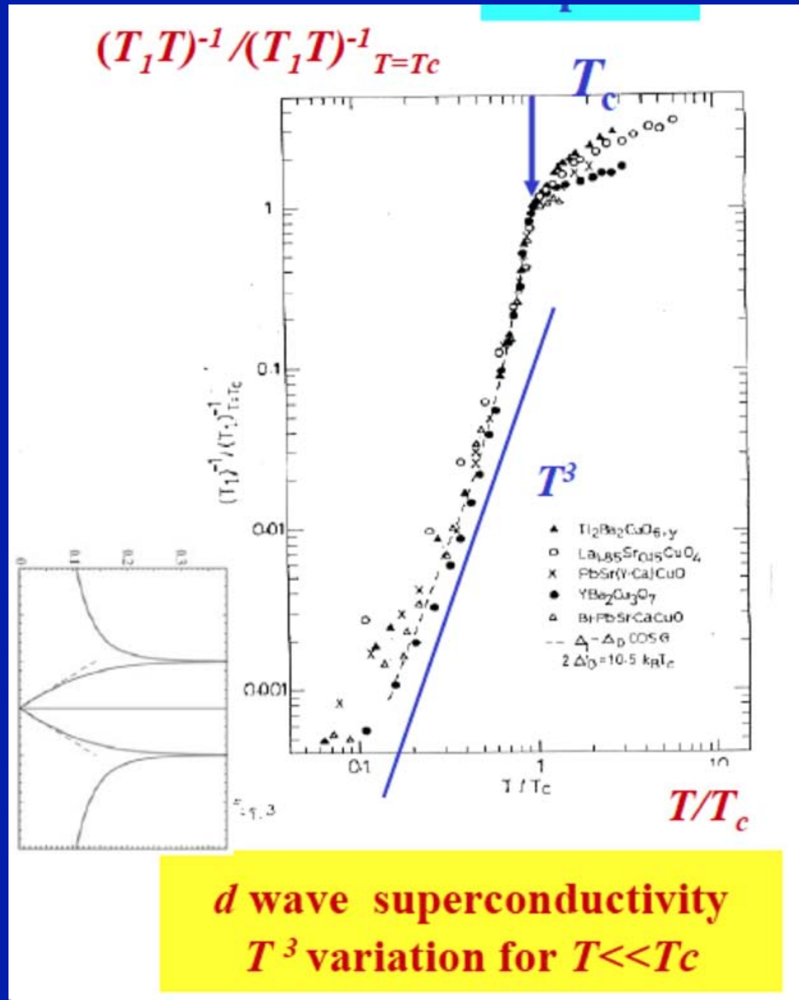

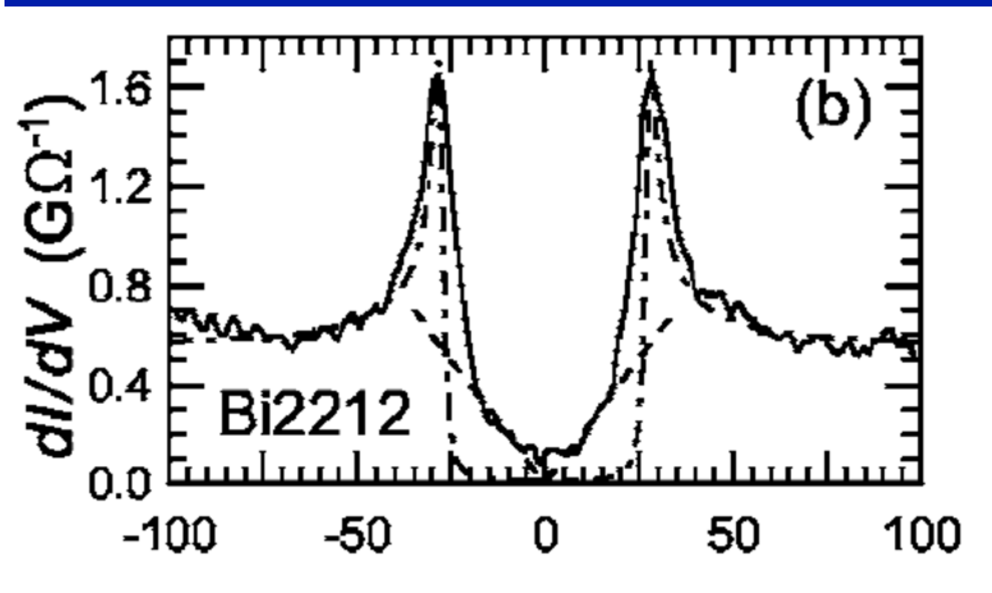

Early STM spectra:
Nodeless s-wave vs. d-wave fits
(cf. C.Berthod's seminar)

ARPES:

magnitude,
not sign
[phase]

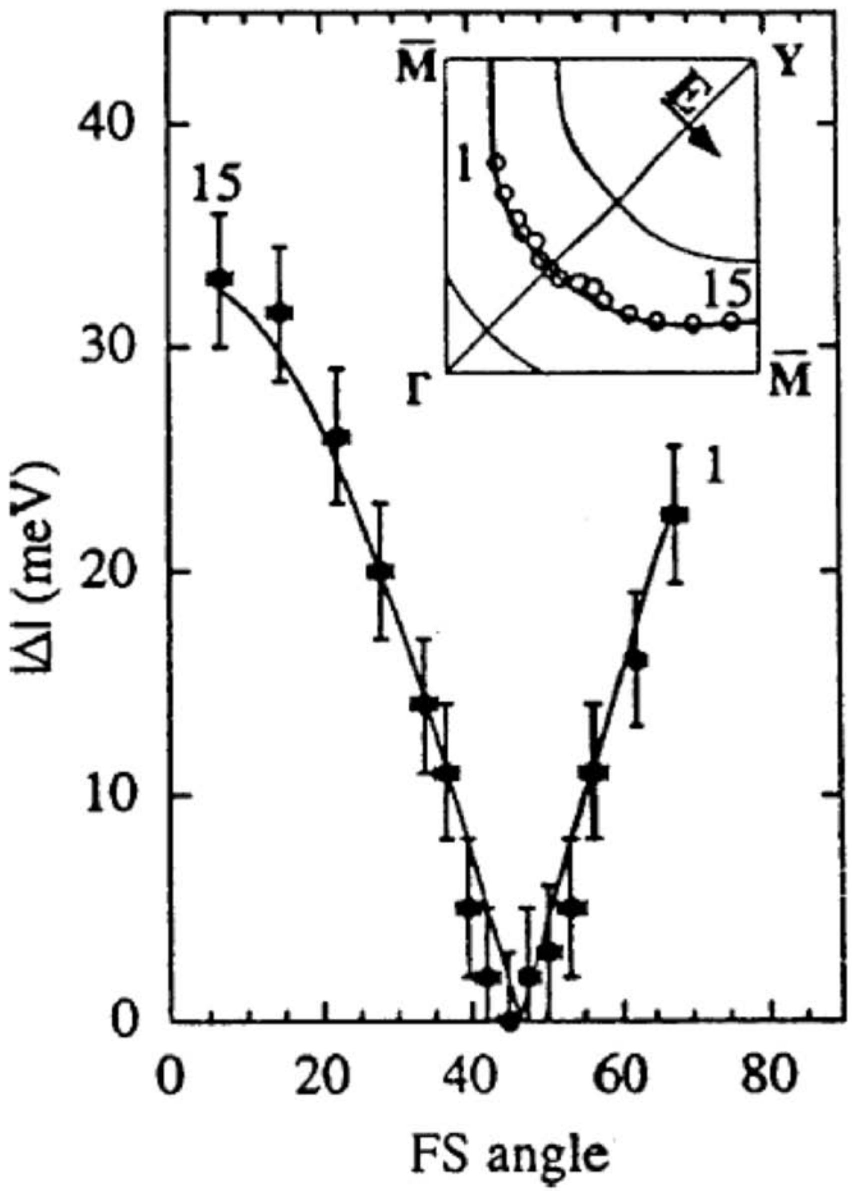

FIG. 4. Energy gap in Bi-2212: ●, measured with ARPES as a function of angle on the Fermi surface; solid curve, with fits to the data using a *d*-wave order parameter. Inset indicates the locations of the data points in the Brillouin zone. From Ding, Norman, *et al.* (1996).

Phase-sensitive experiments: direct test of symmetry

Observation of ½ flux quantum at tricrystal ``π-junctions'' (with odd number of sign changes of I_c)

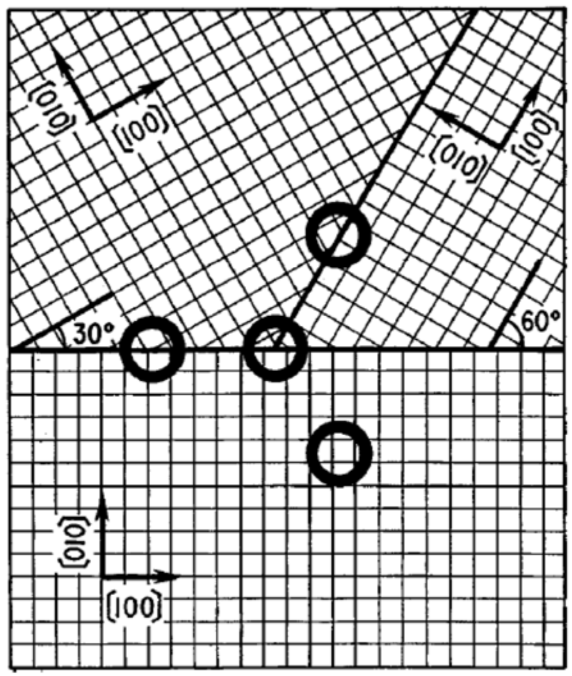

FIG. 11. Experimental configuration for the π-ring tricrystal experiment of Tsuei *et al.* (1994). The central, three-junction ring is a π ring, which should show half-integer flux quantization for a $d_{x^2-y^2}$ superconductor, and the two-junction rings and zero-junction ring are zero rings, which should show integer flux quantization, independent of the pairing symmetry.

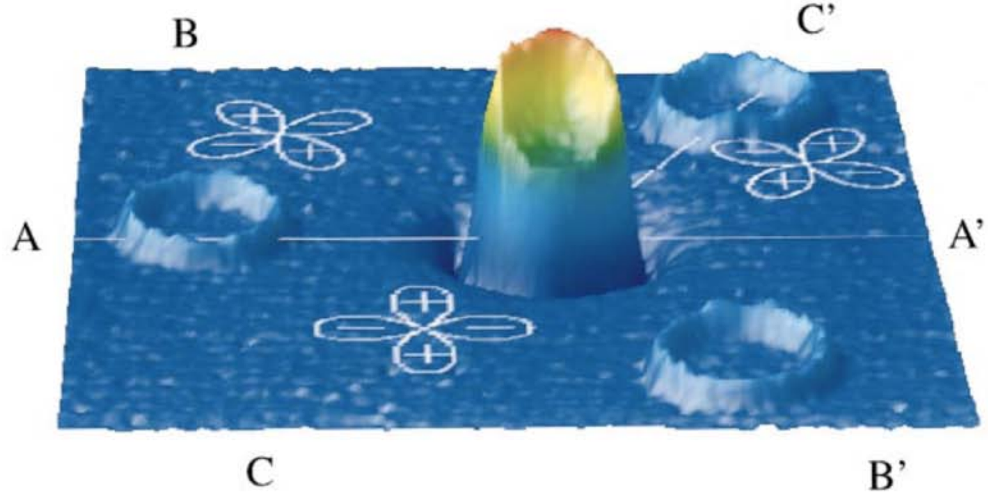

FIG. 13. Three-dimensional rendering of a scanning SQUID microscope image of a thin-film YBCO tricrystal ring sample, cooled and imaged in nominally zero magnetic field. The outer control rings have no flux in them; the central three-junction ring has half of a superconducting quantum of flux spontaneously generated in it [Color].

Effect predicted by Bulaevski (1977),
Geshkenbein and Larkin, 1996; Sigrist and Rice 1992

Reviews: Tsuei and Kirtley, rev Mod Phys (2000)
Kirtley and Tafuri, Handbook of hi-Tc (Springer, 2007)
D. Van Harlingen Rev Mod Phys 67, 515 (1995)

Superfluid density and stiffness

London penetration depth for field perpendicular to layers:

$$\lambda_{\perp}^{-2} = \frac{4\pi e^2}{c^2} \frac{n_s^{3D}}{m^*} \quad , \quad (m^* \simeq 2m)$$

Measurement by muon spin-rotation.

Uemura's empirical relation: $\lambda_{\perp}^{-2} \propto T_c$

At small doping level, $T_c/t \sim x$, hence small superfluid density proportional to the number of doped holes

Remember Drude weight in the normal state, also ~x

In SC state, optical conductivity has a δ-function peak at ω=0, with weight proportional to x.

This implies a small superfluid stiffness…

[cf. Emery and Kivelson, Nature 1995]

Energy cost of a phase twist:

$$\frac{1}{2}K_s\int d^2r(\nabla\theta)^2 = \int d^2r\frac{1}{2}m^*v_s^2 n_s \quad , \quad v_s \propto \frac{\hbar}{m^*}\nabla\theta$$

Hence:

$$K_s = \frac{\hbar^2}{4m^*}n_s^{2D} = \frac{\hbar^2 c_0}{4m^*}n_s^{3D}$$

The proximity of the Mott insulator suppresses the superfluid density and the superfluid stiffness,

both proportional to the number of doped holes

[in agreement with Brinkman-Rice/slave boson/RVB picture]

→ Important to set T_c in UD regime

Low-energy excitations in the SC state: nodal quasiparticles

- Single-particle excitations in the SC state are:
- 1) Pair-breaking (Bogoliubov) quasiparticles excitations away from the nodal points
- 2) Gapless excitations at the nodal points (which control low-temperature/low energy response functions)

Bogoliubov quasiparticles at the antinodes do exist but are fragile

Remember: ARPES antinodal lineshape does not have a sharp quasiparticle in the normal state

A peak is recovered below Tc (`peak-dip-hump' structure) but with a small spectral weight at low doping level

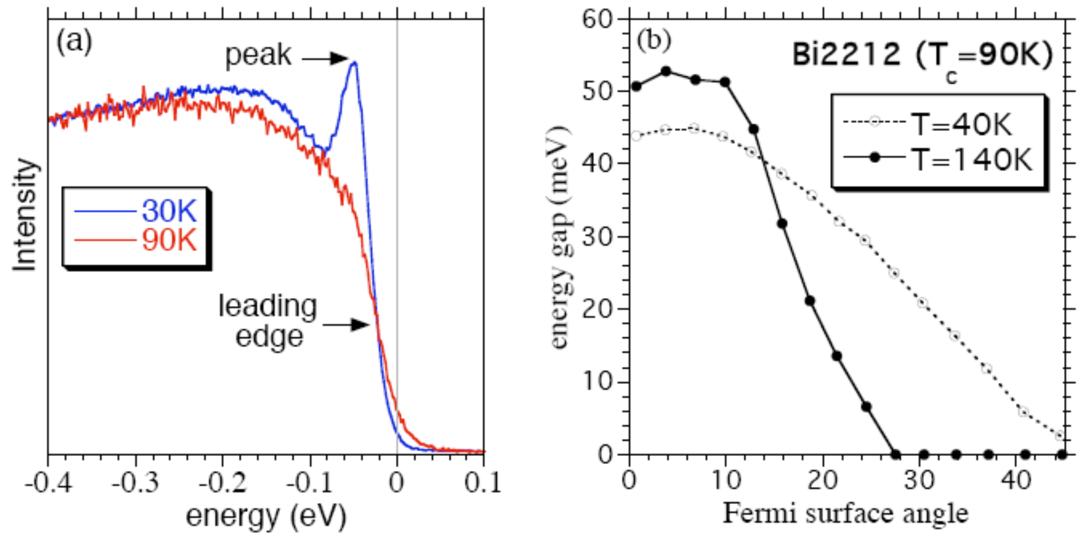

Figure 5 – (a) ARPES spectrum at (π,0) for an underdoped Bi2212 sample in the superconducting state (30K) and the pseudogap phase (90K). The sharp peak in the superconducting state is replaced by a leading edge gap in the pseudogap phase. (b) Angular anisotropy of the superconducting gap (40K) and the pseudogap (140K) for an optimal doped Bi2212 sample. Data courtesy of Adam Kaminski and Juan Carlos Campuzano.

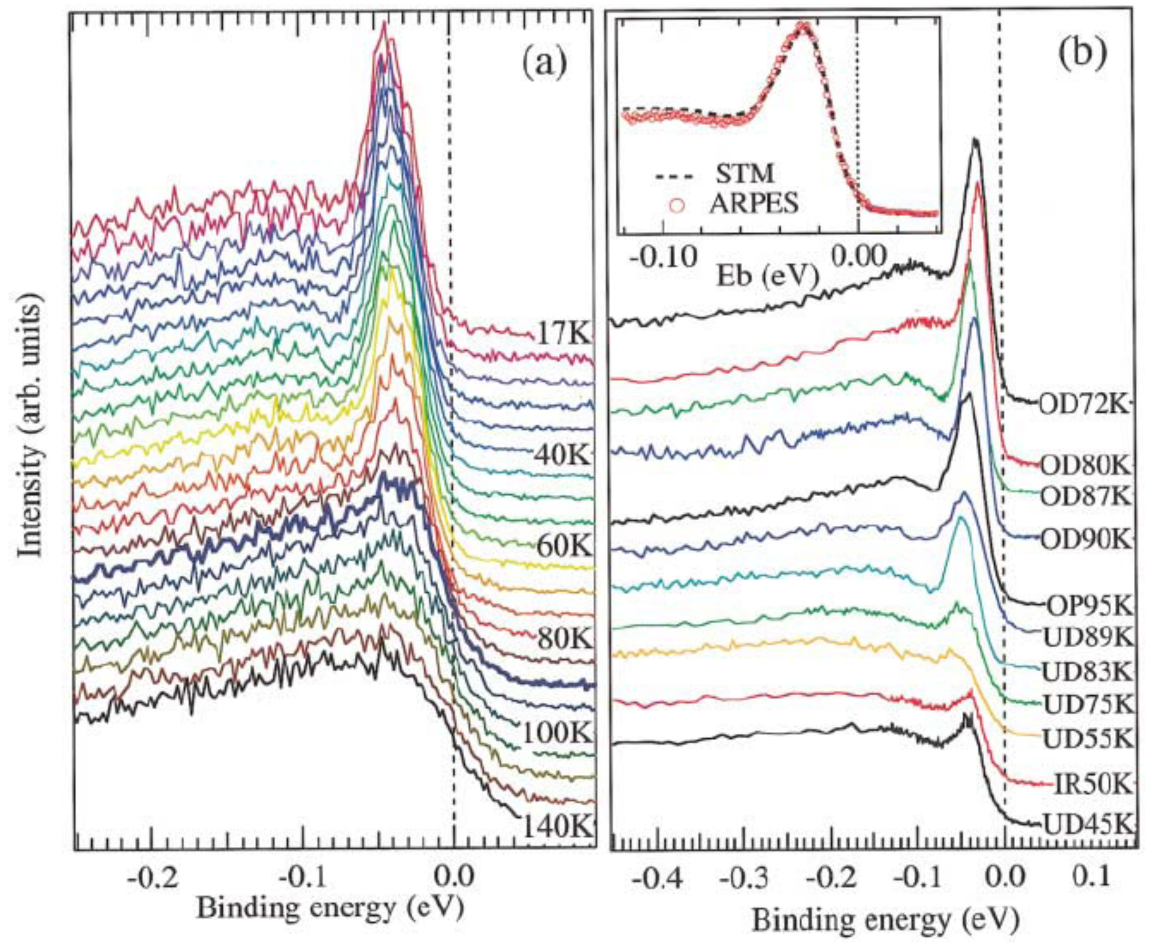

FIG. 1 (color). (a) ARPES spectra at $(\pi, 0)$ of slightly overdoped Bi2212 ($T_c = 90$ K) for different temperatures ($T = 17$, 20, 25, 30, 35, 40, 45, 50, 55, 60, 65, 70, 75, 80, 85, 90, 95, 100, 110, 120, 130, and 140 K). (b) Spectra at $(\pi, 0)$ at low T (14 K) of differently doped Bi2212 samples (OD—overdoped; OP—optimally doped; UD—underdoped; IR—300 MeV electron irradiated, followed by the value of T_c). Intensity of the spectra is normalized at a high binding energy where the spectral intensity shows a minimum (~ -0.5 eV). Inset: Comparison between low-T ARPES at $(\pi, 0)$ and STM for the same OD72K sample.

Ding et al. PRL 87, 227001 (2001)

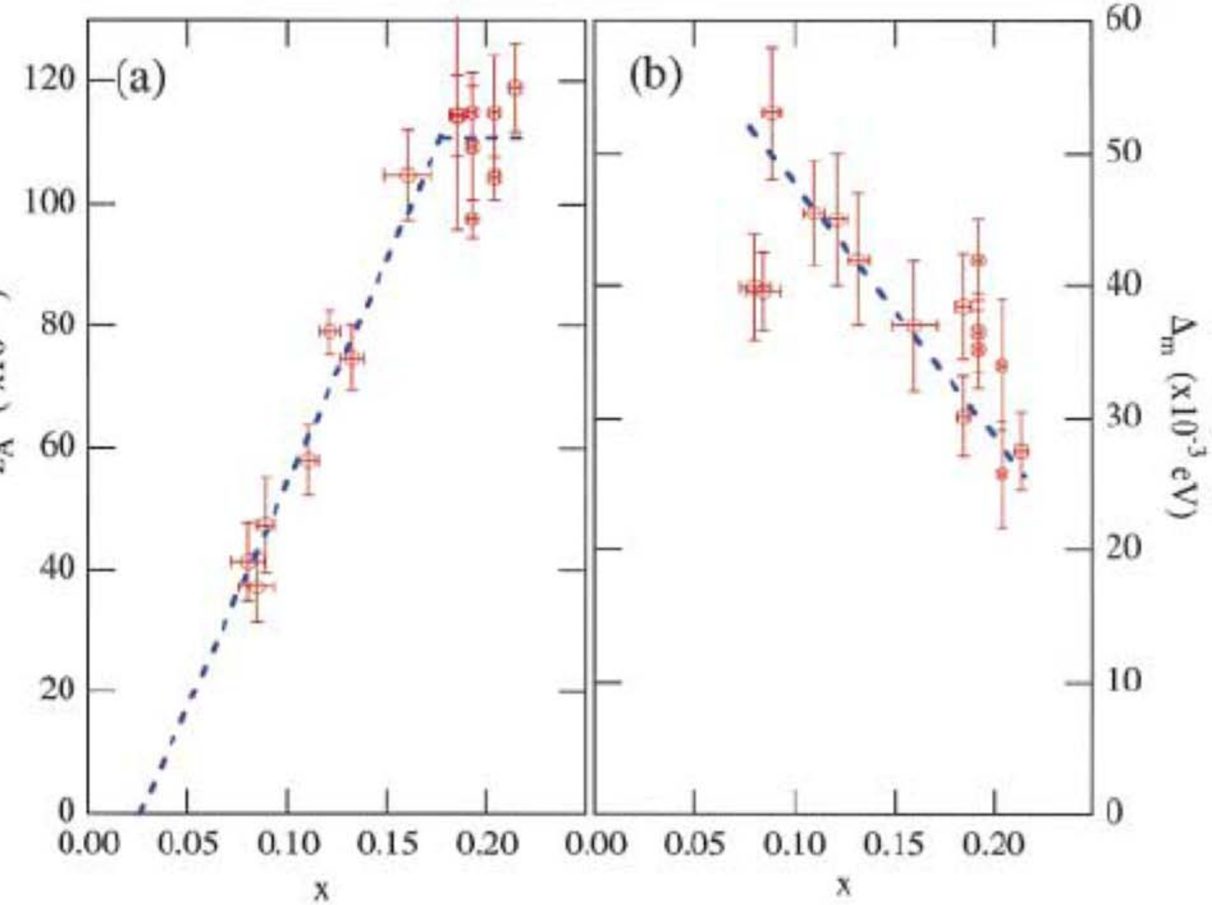

FIG. 3 (color). (a) Doping dependence of the low-T (14 K) coherent weight z_A. The dashed line is a guideline showing that z_A increases linearly on the underdoped side, and tapers off on the overdoped side. (b) Doping dependence of the maximum gap Δ_m at 14 K obtained from the fitted position of the QP peak. Vertical error bars plotted in this and following figures are mostly from fitting uncertainty rather than from measurement. Notice that two heavily underdoped samples (UD45K and IR50K) have smaller gaps. This may be due to the effect of impurities as reflected in their broader transition width.

Existence of AN quasiparticles in the SC at low doping has been a somewhat controversial subject…

Kohsaka et al. Nature (2008):

Quasiparticle interference (STM) in SC state observed only along an \`arc' which is limited

by the AF BZ boundary

Figure 3 | Extinction of BQP interference. **a**, Locus of the Bogoliubov band minimum $\mathbf{k}_B(E)$ found from extracted QPI peak locations $\mathbf{q}_i(E)$, in five independent $Bi_2Sr_2CaCu_2O_{8+\delta}$ samples with decreasing hole density. Fits to quarter-circles are shown and, as p decreases, these curves enclose a progressively smaller area. We find that the BQP interference patterns disappear near the perimeter of a **k**-space region bounded by the lines joining $\mathbf{k} = (0, \pm\pi/a_0)$ and $\mathbf{k} = (\pm\pi/a_0, 0)$. The spectral weights of $\mathbf{q}_2$, $\mathbf{q}_3$, $\mathbf{q}_6$ and $\mathbf{q}_7$ vanish at the same place (dashed line; see also Supplementary Fig. 3). Filled symbols in the inset represent the hole count $p = 1 - n$ derived using the simple Luttinger theorem, with the fits to a large, hole-like Fermi surface shown in Supplementary Fig. 4a and indicated schematically here in grey. Open symbols in the inset are the hole counts calculated using the area

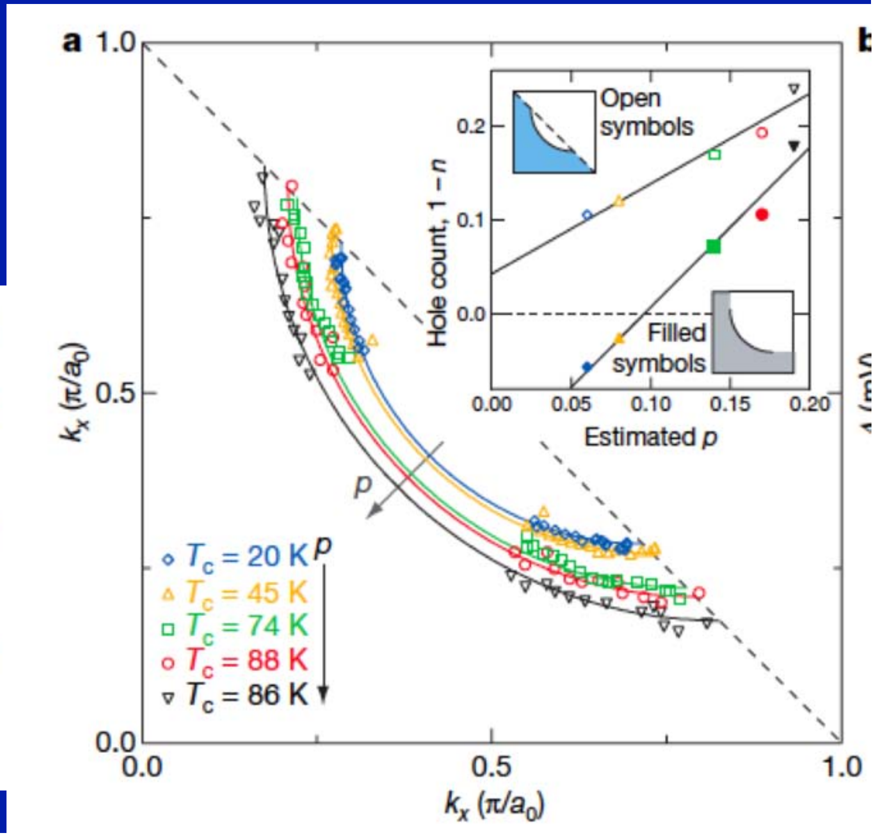

Vishik et al. [Nature Physics, 2009] however suggest that the broadening and spectral weight reduction of the AN-QP observed in ARPES is consistent with the observed disappearance of QP interference

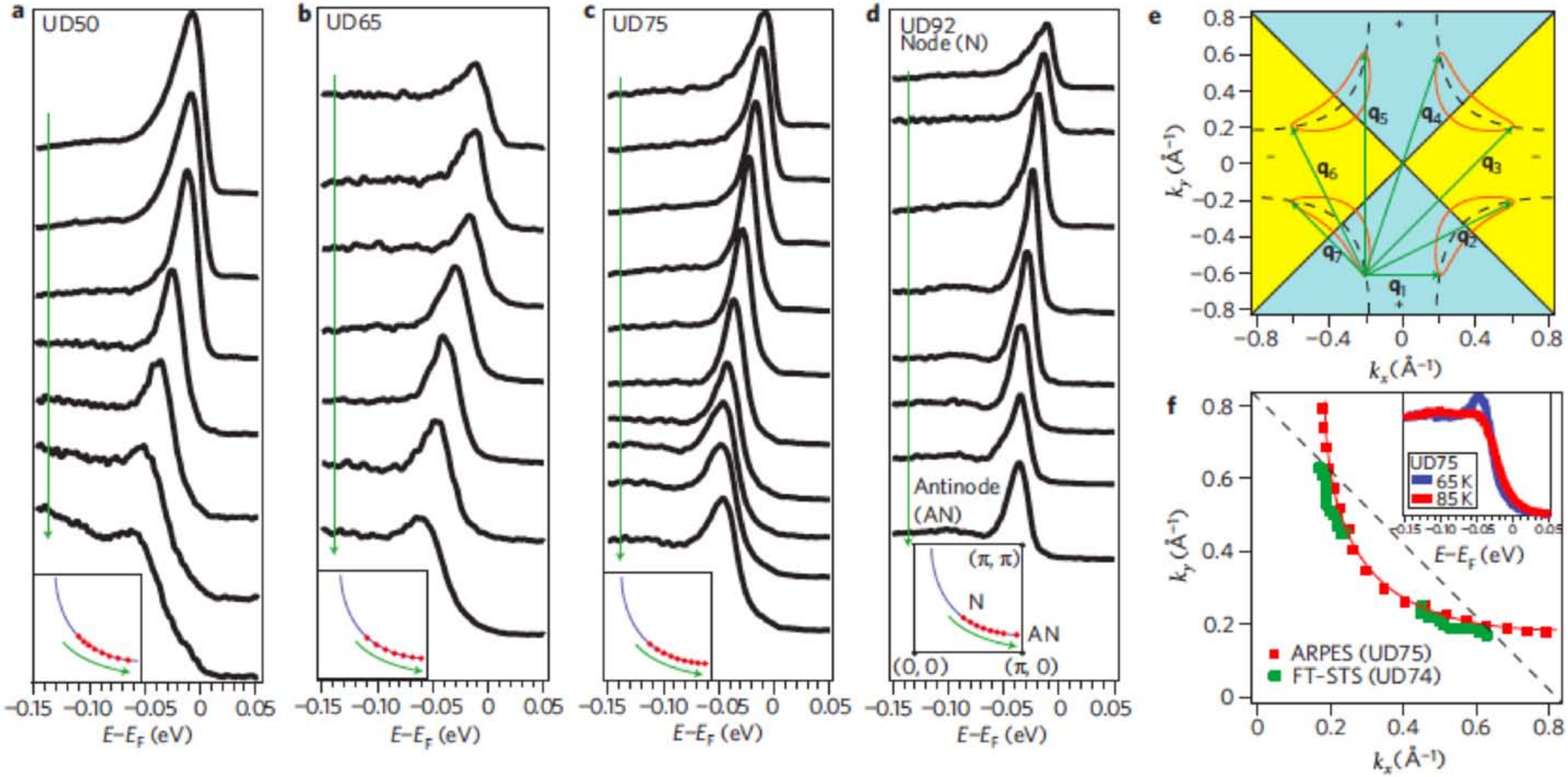

Figure 1 | Quasiparticles in ARPES data. a–d, EDCs at $\mathbf{k}_F$: node (top) to antinode (bottom). Insets: Fermi surface intersection for each cut. **e**, Octet model QPI wave vectors, $\mathbf{q}_1$–$\mathbf{q}_7$, connect the ends of CCEs (red solid lines)[5] around the Fermi surface (dashed line), where blue (yellow) regions represent $\Delta(\mathbf{k}) > 0$ ($\Delta(\mathbf{k}) < 0$). **f**, Fourier-transform (FT) STS infers the Fermi surface by tracking dispersing QPI wave vectors, terminating at the antiferromagnetic zone boundary (dashed line)[5]. For a similar doping, ARPES detects quasiparticles extending to the antinode. Inset: UD75 EDCs at the antinode measured at 85 K and 65 K, showing emergence of the quasiparticle peak near T_c.

AN QPs - Tentative conclusion:

- QPs excitations exist all along the FS in the SC state
- At antinodes, spectral weight is strongly suppressed as well as lifetime at low doping levels
- Hence, the proximity of the Mott insulator state manifests itself <u>also in the SC state</u> by a strong nodal/antinodal dichotomy at low doping

→ See more in Alain Sacuto's seminar

Nodal QPs and low-energy physics of the SC state

- I will heavily use:
- L.Ioffe and A.J. Millis, J. Phys. Chem. Sol. 63, 2259 (2002)
- P.A.Lee and X.G.Wen, PRL 78, 4111 (1997); Wen and Lee, PRL 80, 2193 (1998)
- N. Hussey, Adv. Hys 2002
- M. Le Tacon et al. Nature Physics, 2006

Nodal QPs are characterized by:

- The 2 velocities v_F, v_Δ defining their Dirac-like dispersion.
- Their spectral weight in comparison to all 1-particle excitations, Z_N
- An ``effective charge'' Z_e or Landau parameter defining the coupling to an EM field
- Finally, the EM part of the effective action involves the superfluid stiffness ρ_s

WANTED !

Doping dependence of all these characteristic parameters

[unfortunately,

not yet fully settled experimentally]

Dictionary…

Ioffe-Millis	Lee and Wen	Sacuto et al.
Z_e	α	$Z_N \Lambda$

Low-energy theory:

$$\mathcal{L} = \mathcal{L}_\psi + \mathcal{L}_\phi + \mathcal{L}_{\psi\phi}$$

$$\mathcal{L}_\psi = \sum_{a=1,\cdots,4} \psi_a^+ (\partial_\tau - H_D) \psi_a$$

$$\xi_k^{QP} \simeq \sqrt{v_F^2\, \delta k_{||}^2 + v_\Delta^2 \delta k_\perp^2}$$

$$\mathcal{L}_\phi = \frac{1}{2} \rho_s (\nabla\phi + i2e\vec{A})^2$$

$$\mathcal{L}_{\psi\phi} = \sum_{\alpha,\sigma,p,q} \left(\frac{1}{2} \partial_\mu \phi(r) + ieA_\mu(r) \right) \cdot e^{iq\cdot r} Z_p^{e} \vec{v}_F \psi^+_{p+q/2\alpha\sigma} \psi_{p-q/2\alpha\sigma}$$

Integrate out fermions:
[slowly varying EM field and phase]

$$F_{\text{static}}(\vec{Q}) = \frac{1}{2}\rho_{\text{s}}^{0} Q^2 - 2T \sum_{\alpha} \int \mathrm{d}E N(E) \times \ln\left[1 + \exp\left[-\left(E + \frac{1}{2} Z_p^e \vec{Q}\cdot\vec{v}_a\right)/T\right]\right]$$

$$\vec{Q} \equiv \vec{\nabla}\phi - i2e\vec{A}$$

N(E): linear density of states, cf. above

Specific heat

differentiate twice

w.r.t temperature →

$$\frac{C}{T} = \frac{T}{4\pi v_F v_\Delta} \sum_\alpha \int_0^\infty \mathrm{d}x \frac{x\left(x + \frac{Z_p^e \vec{Q}\cdot\vec{v}_a}{2T}\right)^2}{\cosh^2\left[\frac{x + \frac{Z_p^e \vec{Q}\cdot\vec{v}_a}{2T}}{2}\right]}$$

Zero-field, low-T:

T^2 term

$$\frac{C(B=0)}{T} = \frac{18\zeta(3)T}{\pi v_F v_\Delta}$$

High-field, low-T:

Volovik effect !

$$\frac{C(Z^e vQ \ll T)}{T} = \sum_{\alpha=1,\dots,4} \frac{\pi Z^e}{12 v_F v_\Delta} |\vec{Q}\cdot\vec{v}_a|$$

$$\boxed{\frac{C(B > \Phi_0 v_F^2/T^2)}{T} = \frac{\pi Z^e}{3 v_\Delta}\left(\frac{B}{\Phi_0}\right)^{1/2} A}$$

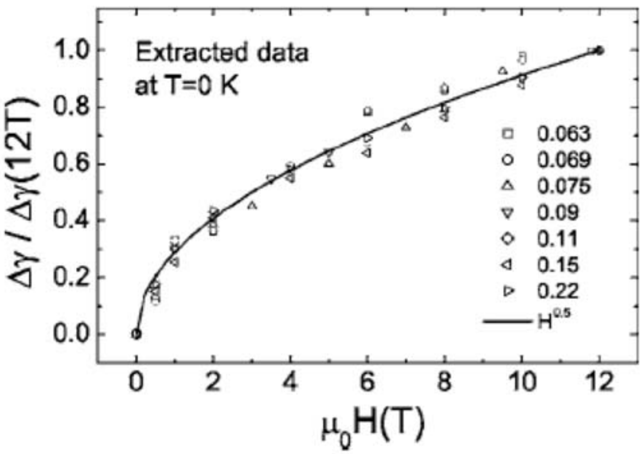

FIG. 2. Field dependence of $\Delta\gamma=[C(H)-C(0)]/T$ normalized by the data at about 12 T in zero temperature limit. It is clear that Volovik's $\sqrt{H}$ relation describes the data rather well for all samples. This indicates a robust *d-wave* superconductivity in all doping regimes.

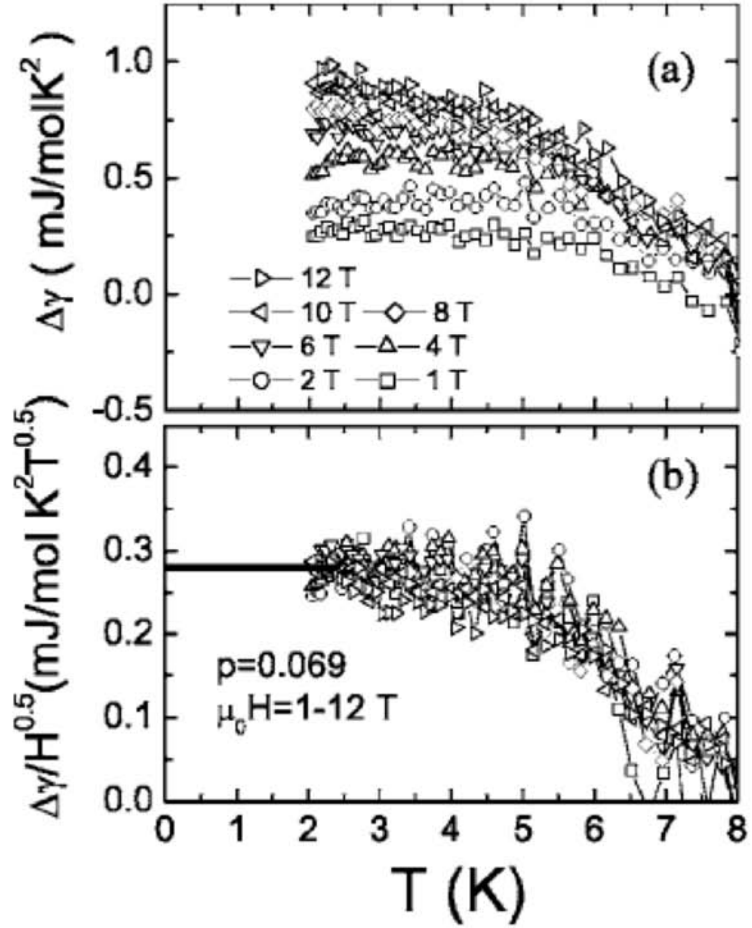

FIG. 3. (a) The typical original data of $\Delta\gamma$ vs. T for the underdoped sample $p=0.069$ at different magnetic fields. (b) The same set of data plotted as $\Delta\gamma/\sqrt{H}$ vs. T. One can clearly see that in zero temperature limit $\Delta\gamma/\sqrt{H}$ is a constant for all fields implying the validity of the Volovik's relation $\Delta\gamma=A\sqrt{H}$. From here one can also determine the value A which is about 0.28 mJ/mol K^2 $T^{0.5}$ as marked by the thick bar.

Experimental observation

[Wen et al. PRB 72 134507 (2005)]

Z_e/v_Δ appears to <u>decrease</u> with underdoping

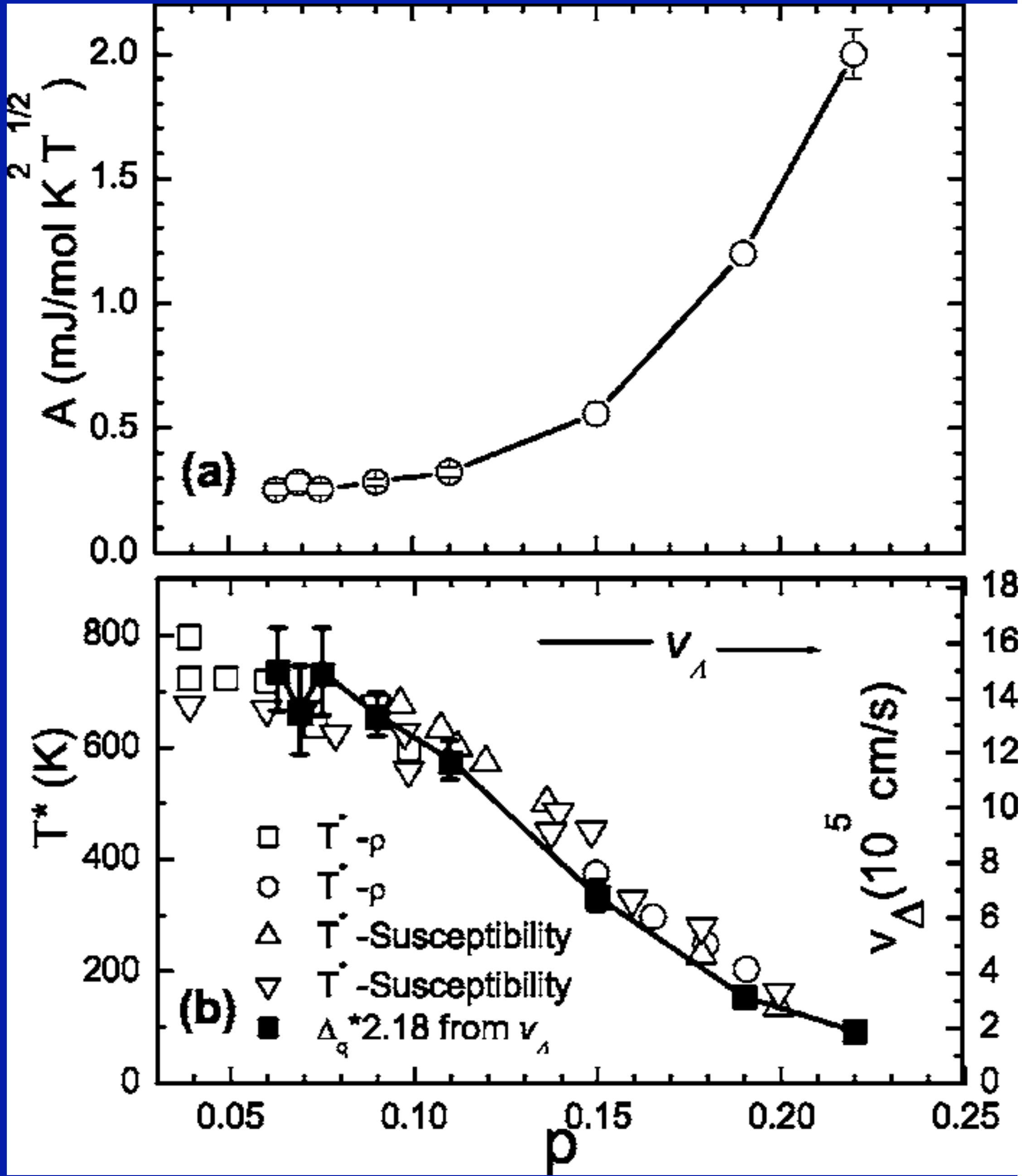

T-dependence of superfluid density/penetration depth

Differentiate F(T,Q) twice w.r.t Q

→

$$\rho_s^{ab} = \rho_{s0}\delta_{ab} - \sum_\alpha \frac{TZ^{e2} v_\alpha^a v_\alpha^b}{4\pi v_F v_\Delta} \int_0^\infty dx \frac{x}{\cosh^2\left[x + \frac{Z^e \vec{Q}\cdot\vec{v}_a}{4T}\right]}$$

$$\boxed{\rho_s(T) = \rho_{s0} - \frac{\ln(2) Z^{e2} v_F}{2\pi v_\Delta} T = \rho_{s0} - \frac{\ln(2) Z^{e2} v_F^2}{36\zeta(3)} \frac{C(B=0)}{T}}$$

Slope: $Z_e^{\,2} v_F / v_\Delta$

Lee and Wen, PRL 1997

Over wide range of intermediate doping, T-linear term in ρ_s is found to be doping-independent

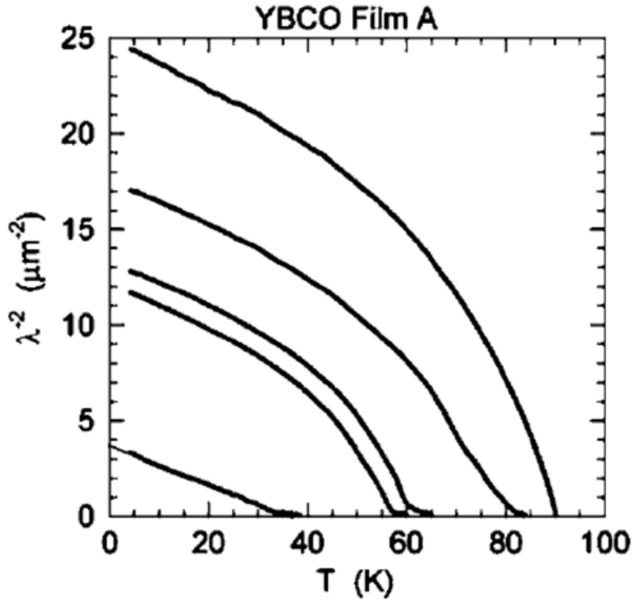

FIG. 14. The London penetration depth measured in a series of YBCO films with different oxygen concentrations and T_c's. The plot shows λ^{-2} plotted vs temperature. Data provided by T. R. Lemberger and published in Boyce *et al.*, 2000.

$$\rho_s(T) = \rho_s(0)\left[1 - c\frac{T}{T_c} + \cdots\right]$$

$$\rho_s(0) \propto T_c$$

Panagopoulos and Xiang, PRL 81, 2336 (1998)

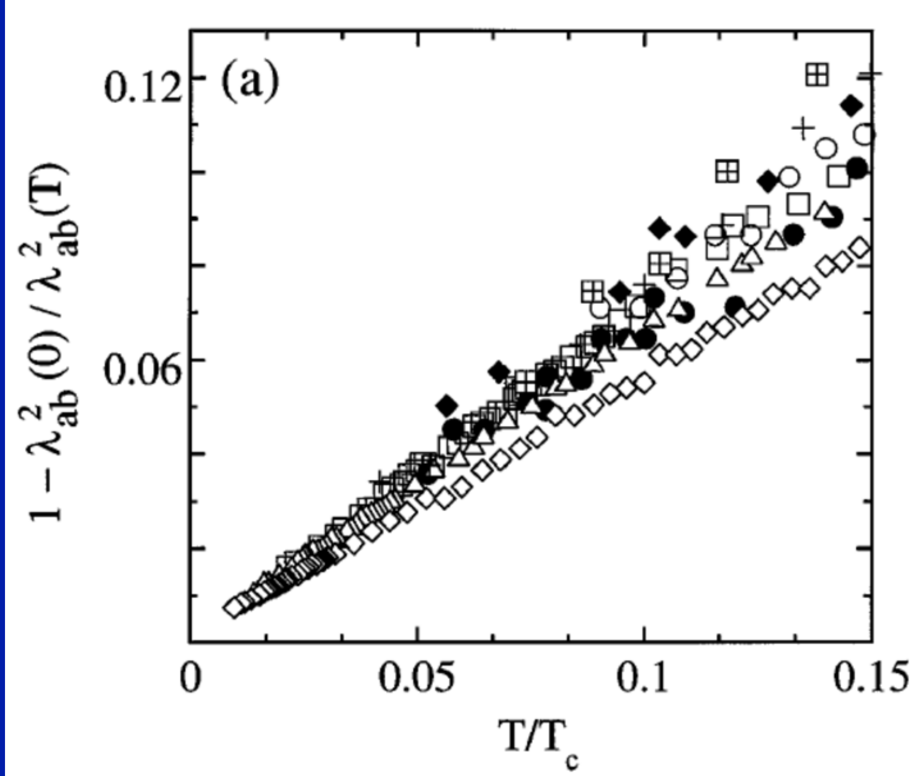

However, at very small doping, doping-dependence of slope is apparently recovered, Uemura `law' modified, but scaling with T/T_c is preserved

$$H_{c1} = \Phi_0[\ln(\kappa) + 0.5]/(4\pi\lambda_{ab}{}^2).$$

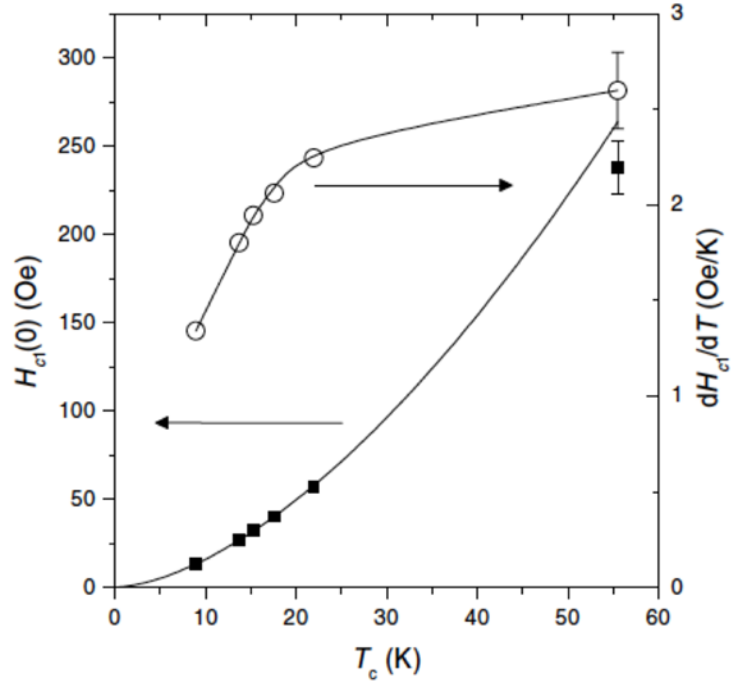

FIG. 3. $H_{c1}(0)$ (solid squares, left scale) and $-dH_{c1}/dT$ (open circles, right scale) as functions of T_c. The curve through the solid squares is the power law fit to the data of $T_c \leq 22$ K, $H_{c1}(0) = 0.366 T_c^{1.64}$ (Oe).

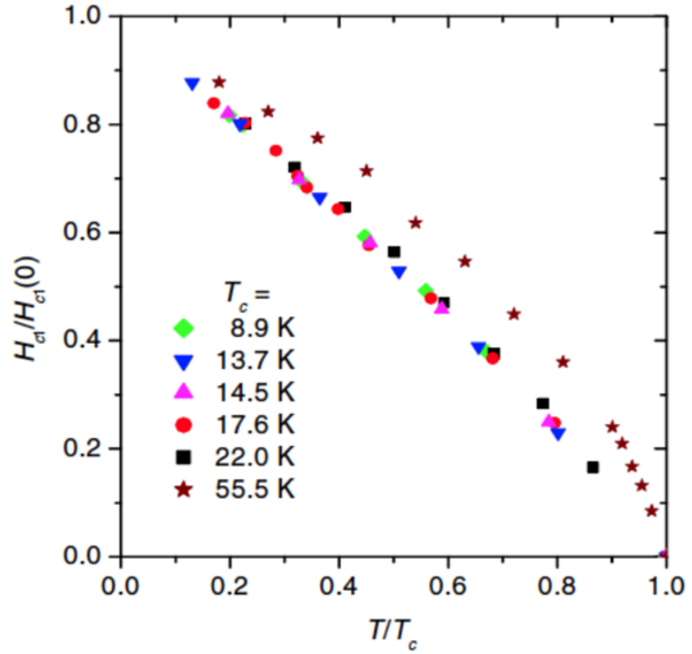

FIG. 4 (color online). Plot of $H_{c1}/H_{c1}(0)$ against reduced temperature T/T_c. All data of $T_c \leq 22$ K fall into a single curve.

Liang et al., PRL 94, 117001 (2005)

High-purity YBCO (UBC samples)

$$\rho_s \sim T_c^{1.64}\left[1 - c\frac{T}{T_c} + \cdots\right]$$

Raman scattering
in B_{2g} (nodal) geometry:
a similar observation
at intermediate doping levels
(~ <u>constant slope</u>)

[Le Tacon et al. Nature Phys 2, 537 (2006)]

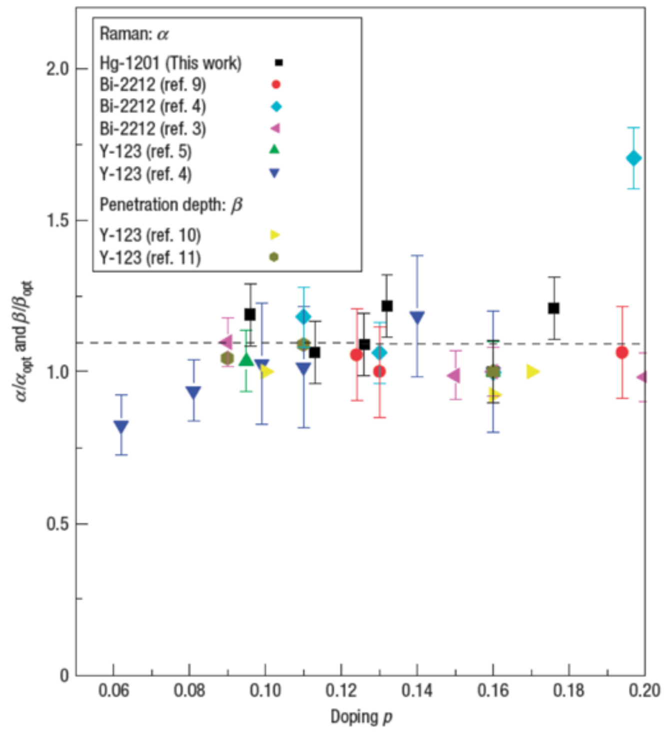

Figure 4 Doping dependence of the low-energy slope α of the nodal (B_{2g}) Raman response ($\alpha = (N_F/v_\Delta)(Z\Lambda)^2_N$), normalized to the optimal doping one ($p = 0.16$). The error bars originate from the linear fitting of this slope from our data and those of refs 3–5,9. The Fermi-liquid parameter $\beta = (N_F/v_\Delta)(Z\Lambda_\rho)^2_N$ extracted from the temperature dependence of the penetration depth[10,11], is also shown. α and β are both found to be doping independent in the range ($p = 0.09$–0.020).

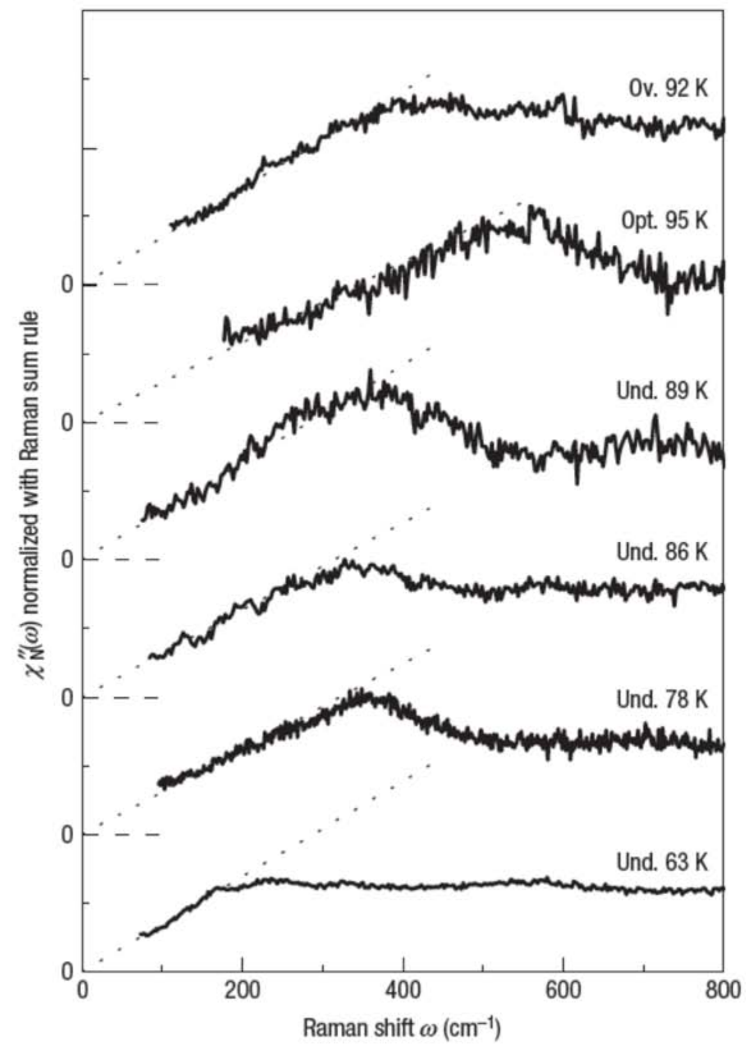

Figure 3 Normalized Raman response functions with respect to the sum rule. A weak linear background coming from spurious luminescence for intermediate doping, independent of the scattering geometry and excitation lines, has been subtracted from raw data before carrying out the normalization (note that without this subtraction the final result is qualitatively similar, that is, the low-energy slope α of the normalized nodal Raman response is found to be doping independent).

The ~ constant slope at intermediate doping is a serious problem for U(1) RVB, Brinkman-Rice, etc…
[Lee, Wen]

In those theories (uniform along FS):

- v_Δ *increases* as doping is reduced
- Effective charge Z_e coincides with Z : proportional to doping

Hence, the slope should strongly decrease as doping is reduced
→ Inconsistent with experiments !

To summarize:

- As doping is reduced from optimal:
- From Volovik effect, Z_e/v_Δ decreases
- From $\lambda(T)$ and Raman, $Z_e^2\, v_F/v_\Delta$ is ~ constant and eventually decreases at very low doping
- → At least for not too low doping, it seems reasonable to conclude (assuming v_F weakly dep. on doping) that both Z_e and v_Δ <u>increase</u> as doping is reduced

$$\frac{Z_e}{v_\Delta} \sim T_c^\alpha \;,\;\; \frac{Z_e^2}{v_\Delta} \sim \mathrm{const.}$$

$$\Rightarrow Z_e \sim 1/T_c^\alpha \,,\, v_\Delta \sim 1/T_c^{2\alpha}$$

Consistency with thermal conductivity ?

- Universal clean-limit ?
  [Graf et al, PRB 1996; Durst and Lee, PRB 2000]

$$\frac{\kappa}{T} = \frac{k_B^2}{3\hbar}\frac{n_p}{d_c}\left[\frac{v_F}{v_\Delta} + \frac{v_\Delta}{v_F}\right]$$

- Sutherland et al. PRB (2003)

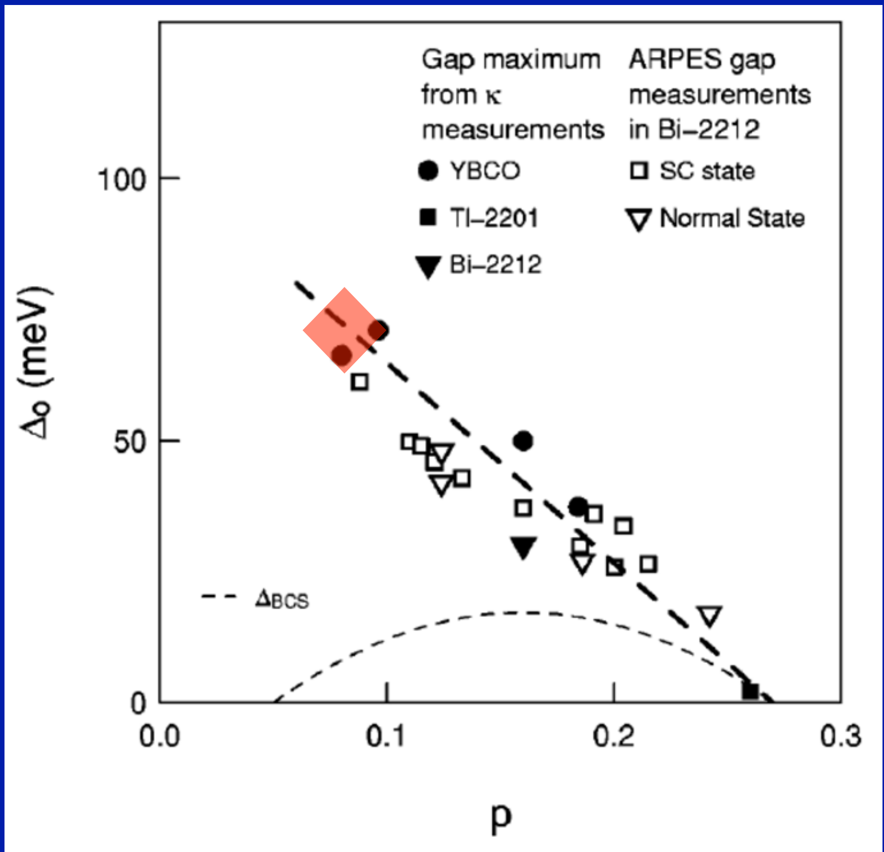

FIG. 6. Doping dependence of the superconducting gap Δ_0 obtained from the quasiparticle velocity v_2 defined in Eq. (3) (filled symbols). Here we assume $\Delta = \Delta_0 \cos 2\phi$, so that $\Delta_0 = \hbar k_F v_2/2$, and we plot data for YBCO alongside Bi-2212 (Ref. 7) and Tl-2201 (Ref. 8). For comparison, a BCS gap of the form $\Delta_{BCS} = 2.14 k_B T_c$ is also plotted, with T_c taken from Eq. (1) (and $T_c^{max} = 90$ K). The value of the energy gap in Bi-2212, as determined by ARPES, is shown as measured in the superconducting state[29] and the normal state[30–32] (open symbols). The thick dashed line is a guide to the eye.

Validity of clean limit questioned by Ando et al

[Sun et al. PRL 2006]

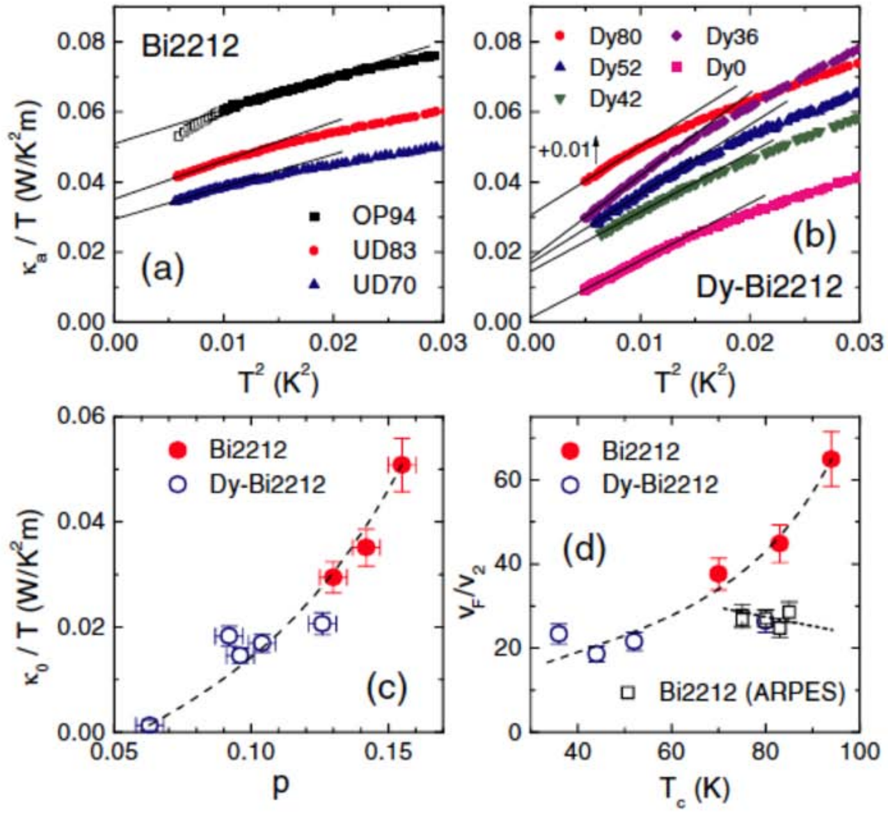

FIG. 3 (color online). (a),(b) a-axis thermal conductivity of Bi2212 and Dy-Bi2212 at low T; Dy80 data are shifted up by 0.01 W/K^2 m for clarity. The solid lines are linear fits to extract κ_0/T. (c) Hole-doping dependence of κ_0/T in Bi2212. (d) The gap parameter v_F/v_2, calculated from κ_0/T using Eq. (1), as a function of T_c in the underdoped region; also shown is v_F/v_2 obtained from ARPES [31] for comparison. The dashed and dotted lines are guides to the eyes.

Two energy scales are observed in in the SC phase
[Le Tacon et al., Nature Phys 2006: see A.Sacuto's seminar]
→ does that mean that 2 scales enter the SC gap
(with different doping dependence) ?

d-wave symmetry does not imply that only the lowest harmonics $\cos k_x - \cos k_y$ is involved, for example:

$$\Delta(\phi) = \Delta_m \left[B \cos 2\phi + (1 - B) \cos 6\phi\right]$$

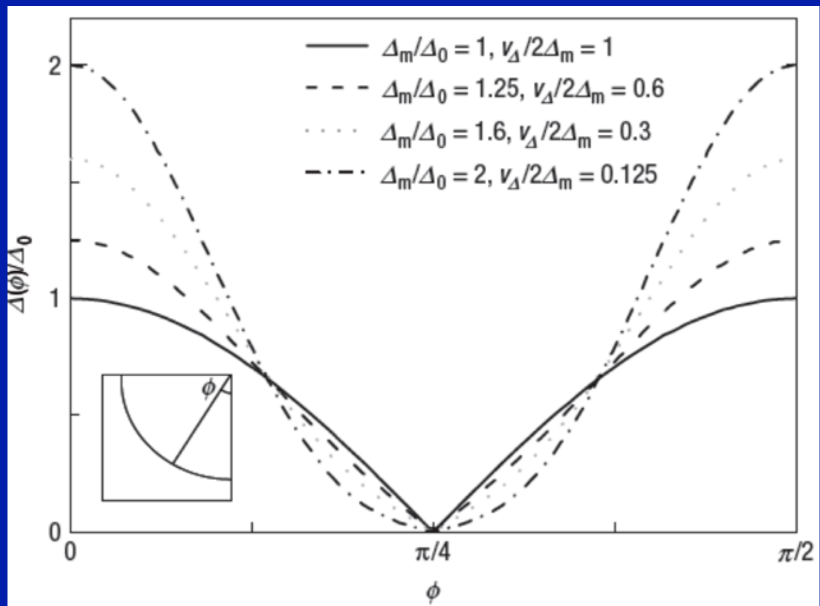

Early observation in favor of 2-scale gap: Tunneling vs. Andreev [G.Deutscher, Nature 1999]

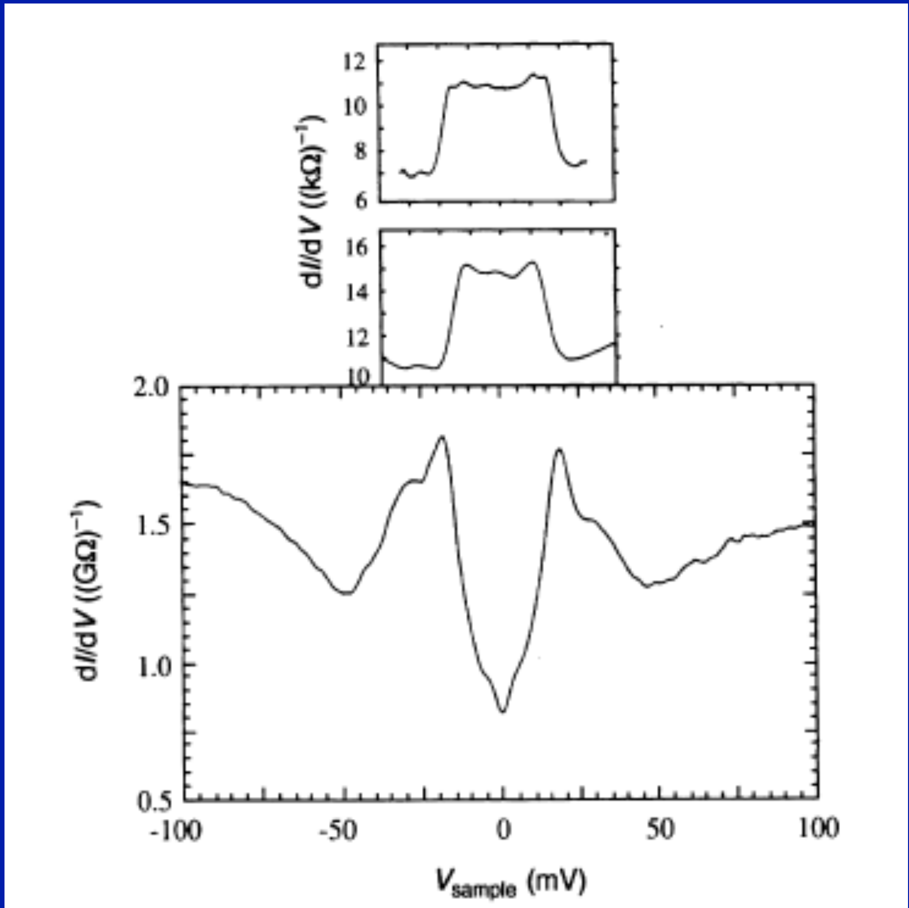

Optimal doping YBCO

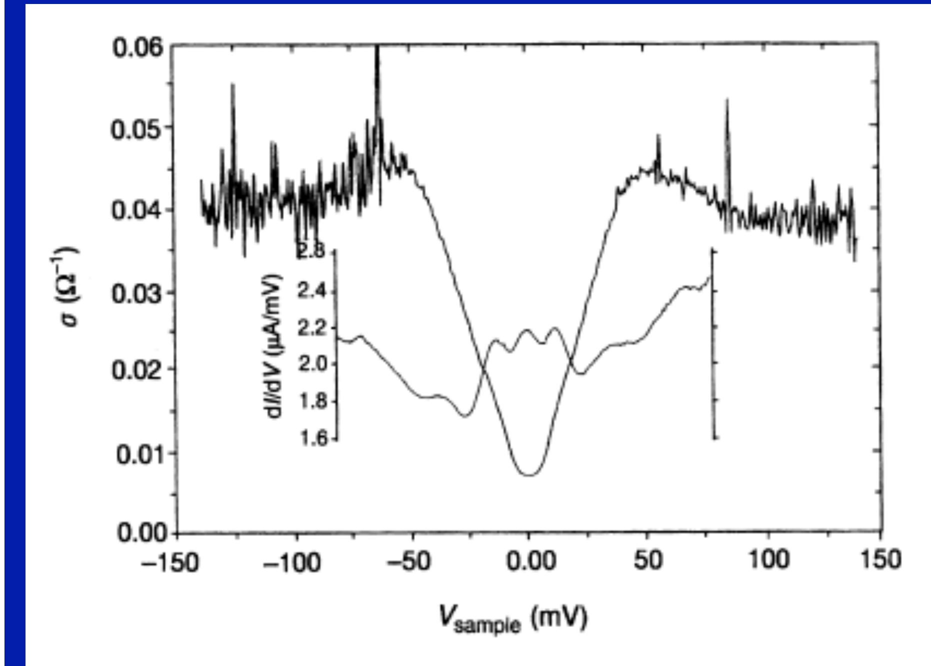

Underdoped YBCO

Also, hint from optics on PCCO: Lobo et al. EPL 2001

Previous hint of 2 energy scales in SC state from ARPES: U-shaped gap

Mesot et al, 1999; Borisenko et al, 2002

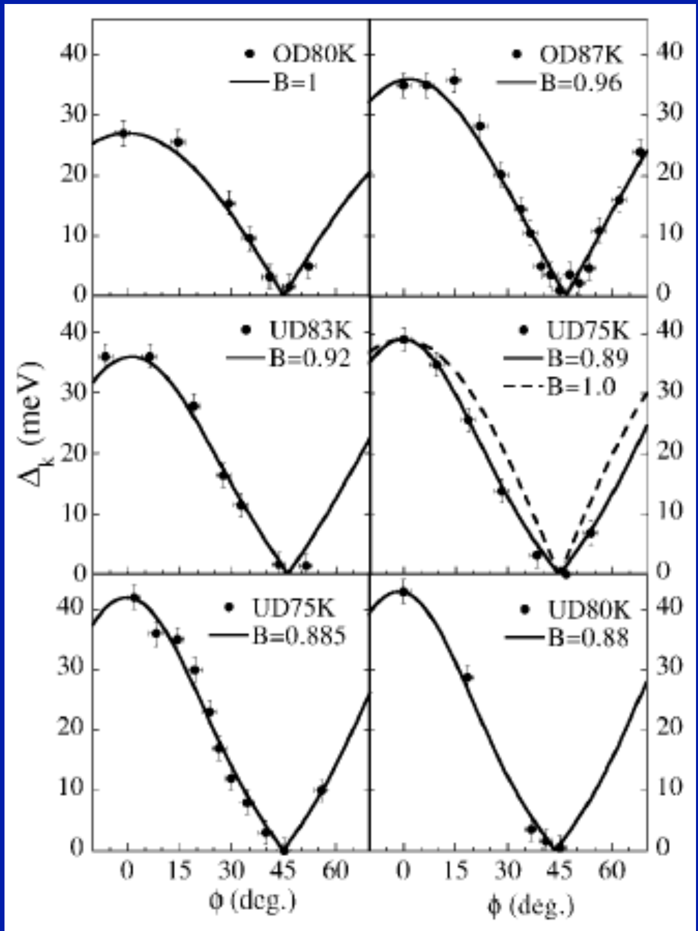

Mesot et al.

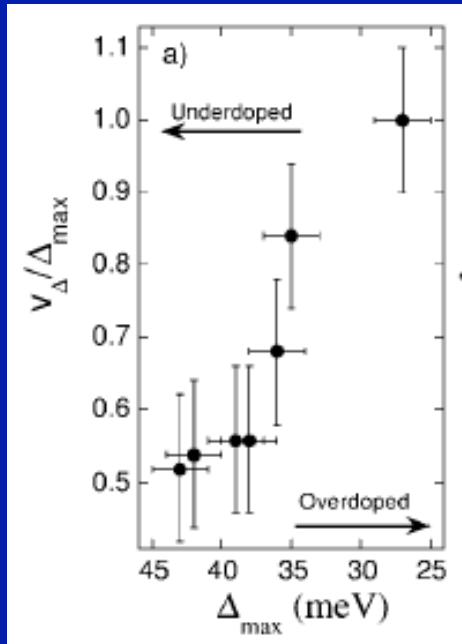

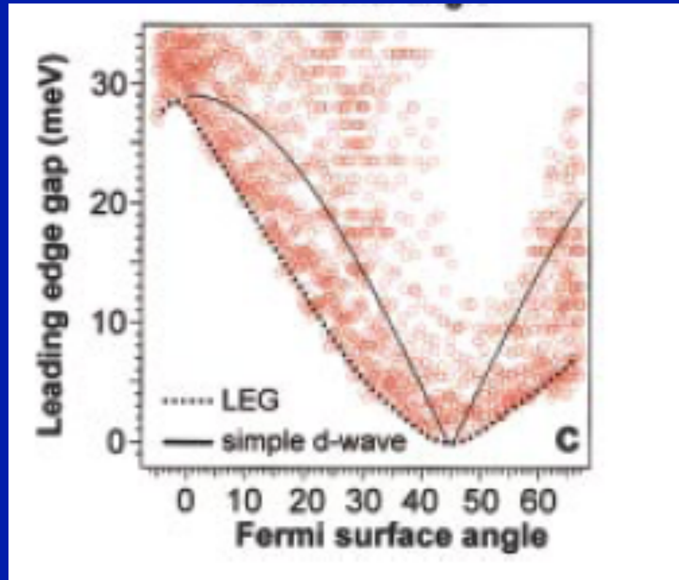

Borisenko et al,

underdoped Bi2212

FIG. 2. Values of the superconducting gap as a function of the Fermi surface angle ϕ obtained for a series of Bi2212 samples with varying doping. Note two different UD75K samples were measured, and the UD83K sample has a larger doping due to aging [16]. The solid lines represent the best fit using the gap function: $\Delta_k = \Delta_{max}[B\cos(2\phi) + (1 - B)\cos(6\phi)]$ as explained in the text. The dashed line in the panel of an UD75K sample represents the gap function with $B = 1$.

Two important topics that I haven't had time to address in this lecture…

- Energetics: kinetic-energy driven transition [in contrast to BCS] !

[Lobo, Bontemps et al. EPL 55, 854 (2001)

Molegraaf et al., Science 295, 2239 (2002)]

- Materials dependence of T_c: dependence on number of CuO_2 layers, t'/t, distance of apical oxygens, etc…

→ Perhaps last session, Dec 14 ?

To conclude … (but unfinished story)

- The UD superconducting phase is NOT conventional BCS
- Proximity to Mott insulator has consequences also for the SC phase at low doping
- Nodal/Antinodal dichotomy persists in UD SC phase → partial suppression of Bogoliubov QP coherence at antinodes